



## **Batch Adsorption Study and Kinetic Profile of Cr(VI) Using Lumbang (*Aleurites moluccana*)-Derived Activated Carbon-Chitosan Composite Crosslinked With Epichlorohydrin**

**NELSON R. VILLARANTE<sup>1</sup>, ANGELO PATRICK R. BAUTISTA<sup>1</sup>  
and DERICK ERL P. SUMALAPAO<sup>2,3,4,\*</sup>**

<sup>1</sup>Department of Physical Sciences and Mathematics, College of Arts and Sciences, University of the Philippines Manila, Padre Faura Street, Manila, Philippines.

<sup>2</sup>Department of Biology, College of Science, De La Salle University, 2401 Taft Avenue, Manila, Philippines.

<sup>3</sup>Mathematics Area, School of Multidisciplinary Studies, De La Salle-College of Saint Benilde, 2544 Taft Avenue, Manila, Philippines.

<sup>4</sup>Department of Medical Microbiology, College of Public Health, University of the Philippines Manila, 625 Pedro Gil Street, Manila, Philippines.

\*Corresponding author E-mail: derick.sumalapao@dlsu.edu.ph

<http://dx.doi.org/10.13005/ojc/330307>

(Received: March 30, 2017; Accepted: May 06, 2017)

### **ABSTRACT**

Batch adsorption of toxic Cr(VI) ion from an aqueous solution using lumbang (*Aleurites moluccana*) activated carbon-chitosan composite crosslinked with epichlorohydrin as an adsorbent was investigated. The adsorption experiments were performed at varying pH, agitation time, initial Cr(VI) ion concentration, temperature, and adsorbent dose. At an initial concentration of 60 ppm Cr(VI), the maximum adsorption was observed at pH 3, adsorbent dose of 3 g/L, contact time of 75 min, and temperature of 30 °C. Analysis of the experimental data using different kinetic models revealed that the biosorption phenomenon behaved under a pseudo second-order rate mechanism.

**Keywords:** Biosorption, *Aleurites moluccana*, Chromium, Kinetics, Carbon-chitosan composite, Epichlorohydrin

### **INTRODUCTION**

Humans have been using heavy metals such as mercury in gold mining<sup>1</sup>, arsenic in wood

preservatives and insecticides<sup>2</sup>, and tetraethyl lead as primary antiknocking agent in petrol or automotive gasoline<sup>3</sup>. Subsequently, these heavy metals contaminate various water resources posing several adverse health effects to humans and the

environment. There is an increasing trend in heavy metal exposure globally, particularly in the less developed countries, with a decline in heavy metal emissions in most developed countries over the last century<sup>4</sup>. One of the heavy metals and pollutants present in wastewater is chromium, specifically Cr(VI), which is the focus of this study. Cr(VI) compounds are powerful oxidizing agents<sup>5</sup>, are irritating and corrosive, and appear to be much more toxic systemically than Cr(III) compounds, given similar amounts and solubilities<sup>6</sup>. Once ingested beyond the maximum concentration (0.1 mg/L), chromium can induce vomiting and hemorrhage<sup>7</sup> with its high toxicity attributed to its ease in passing through cell membranes. Endogenous reducing agents such as hydrogen peroxide (H<sub>2</sub>O<sub>2</sub>), glutathione (GSH), and ascorbic acid can produce reactive intermediates such as Cr(V), Cr(IV), thiylradicals, hydroxyl radicals, and Cr(III) which disrupt membrane integrity leading to cellular dysfunction<sup>8</sup>.

Heavy metals are emitted to the environment via different processes and pathways<sup>9</sup> leading to environmental pollution. Bioremediation, the utilization of naturally occurring microorganisms to break down environmental pollutants, has been an emerging field of study. Currently, several processes are employed in the removal of toxic metal ions such as ion exchange, membrane processes, precipitation, and adsorption<sup>10</sup>. Adsorption is recognized as an efficient and economic method for the removal of pollutants from wastewater<sup>11</sup>. However, innovations have been developed involving this process such as the utility of low-cost biosorbents as these can reduce the cost of an adsorption system significantly<sup>12</sup>. Over the past years, biosorption has drawn more attention among scientists because of the diversity of the readily available sorbent material. These adsorbents can be coated by chitosan, obtained from the deacetylation of the natural biopolymer chitin found in crustaceans, insects, and fungal cell walls, and can adsorb dyes, heavy metal ions, and proteins<sup>13</sup>. Furthermore, other properties of chitosan such as its abundance, hydrophilicity, non-toxicity, biodegradability, biocompatibility, and antimicrobial properties make it very useful and effective in water remediation<sup>14</sup>. Hence, this study aimed to remove Cr(VI) ions in water samples using chitosan-activated carbon-epichlorohydrin composite with the outer shells of lumbang (*Aleurites moluccana*) used for activated carbon generation. This study focused on the adsorption of Cr(VI) by low-cost preparation of

activated carbon-chitosan composite crosslinked with epichlorohydrin on synthetic waste water at varying pH, contact time, adsorbent dosage, metal ion concentration, and temperature as an efficient, economic, and environment-friendly biosorbent for the removal of Cr(VI) in aqueous solutions. With pollution of surface water by toxic heavy metals from industrial sources being a serious environmental concern, this study offered useful applications in industries producing high concentrations of heavy metal ions as wastes and a useful alternative method in the reduction of agricultural wastes in the treatment of contaminated aquatic environments.

## MATERIALS AND METHODS

### MATERIALS

Lumbang (*Aleurites moluccana*) seeds were collected from the College of Forestry, University of the Philippines Los Baños, Laguna, Philippines. Chitosan with minimum deacetylation of 75% and epichlorohydrin were purchased from Sigma-Aldrich. Stock solution of 1000 ppm Cr(VI) was prepared by dissolving 0.424 g of K<sub>2</sub>Cr<sub>2</sub>O<sub>7</sub> in deionized water.

### Preparation of Biocharcoal

The shells of *Aleurites moluccana* were separated from the nut and washed several times, subsequently sun-dried for 24 h and crushed into small pieces. Pyrolysis was carried out by traditional burrow method performed in Barangay Banay-Banay, Padre Garcia, Batangas, Philippines. This was done by making a shallow burrow in an open field, the shells were incinerated and covered with soil to prevent the entry of oxygen. The pyrolysis set up was maintained for 5 hours. The resulting charcoal was cooled, collected, washed thoroughly with deionized water and was further pulverized into a particle size between 0.149 to 0.250 mm.

### Preparation of Low Cost Activated Carbon

The charcoal produced was soaked in 25% CaCl<sub>2</sub> for 24 hours for the activation process. The activated biocharcoal was washed thoroughly with deionized water and oven-dried at 100 °C for 6 hours.

### Preparation of Lumbang-Derived Activated Carbon-Chitosan Composite Crosslinked with Epichlorohydrin

Activated carbon was coated with chitosan<sup>15, 16</sup>. Twenty-five grams (25 g) of chitosan

was added to 1 L of 0.4 M oxalic acid solution under continuous stirring at temperature between 45-50 °C. Fifty grams (50 g) of the activated biocharcoal was added to the solution and was mixed thoroughly by a mechanical blender for 2 h. The resulting slurry was oven-dried at 100 °C for 24 h. The dried composite was pulverized using manual grinder to a size of 0.250-0.420 mm. The pH of the composite was adjusted to neutrality and oven-dried again. The pulverized composite was crosslinked by mixing it into a neutral solution of 40 mM epichlorohydrin with continuous stirring maintained at 50 °C.

#### Quantification of Chromium Concentration

Cr(VI) concentration was determined quantitatively<sup>17</sup> by first complexing the Cr(VI) with 1,5-diphenylcarbazide in acidic condition to generate a purple-violet colored complex<sup>5</sup> and then analyzed using UV-Vis spectrophotometer (Perkin Elmer Lambda 2000) set at 540 nm.

#### Batch Adsorption Experiments

Initial concentration of Cr(VI) was introduced into a 15-mL conical tubes where an appropriate amount of adsorbent with a particle size of 0.149 to 0.250 mm was added. To determine the optimal conditions, parameters such as pH, initial concentration, temperature, contact time, adsorbent dosage were varied<sup>18</sup>. Adsorption experiment set ups were done in triplicates, with agitation and incubation performed using SHZ-82A water bath.

#### Effect of pH

The effect of pH on the adsorption ability of the composite was done by introducing 5 mL of Cr (VI) (50 ppm) into 15-mL conical tubes containing the composite (5 g/L). Microcosms with pH ranging from 2-8 were agitated at 160 rpm and the adsorption of the metal was monitored at 30 °C for a period of 180 min.

#### Effect of Contact Time

For the effect of contact time, microcosms were prepared containing adsorbent (5 g/L) and Cr (VI) (50 ppm). Adsorption study was monitored every 15 min for a period of 105 min at a fixed agitation rate of 160 rpm, pH of 3, and temperature of 30 °C.

#### Effect of Temperature

The same preparation was made, except for the varying temperature conditions. The microcosm was maintained at pH 3 and incubated at different temperatures (30-50 °C) for a period of 75 min.

#### Effect of Cr (VI) Concentration

Metal solutions with varying concentrations (10-120 ppm) were prepared and adsorption studies were conducted at fixed agitation rate (160 rpm), adsorbent dose 3 g/L, contact time 75 min, and temperature 30 °C.

#### Effect of Adsorbent Dosage

Microcosms with different adsorbent

**Table 1: Nonlinear and linearized forms of the adsorption kinetic models**

Kinetic Model	Nonlinear Model	Linearized Form
Zero-order	$dq_t/dt=c_0$	$q_t=c_0t+q_0$
First-order	$dq_t/dt=c_1q_t$	$\log q_t=\log q_0+c_1/2.303 t$
Second-order	$dq_t/dt=c_2q_t^2$	$(-1)/q_t=c_2 t+((-1)/q_0)$
Pseudo first-order	$dq_t/dt=c_3(q_e-q_t)$	$\log(q_e-q_t)=\log q_e-c_3/2.303 t$
Pseudo second-order	$dq_t/dt=c_4(q_e-q_t)^2$	$t/q_t=1/(c_4 q_e^2)+1/q_e t$
Elovich	$dq_t/dt=\alpha e^{-\beta t}$	$q_t=1/\beta \ln(\alpha\beta)+1/\beta \ln t$
Intraparticle diffusion	$q_t=k_{id}t^{1/2}+k_0$	$q_t=k_{id} t^{1/2}+k_0$

$q_t$  (mg g<sup>-1</sup>) is the amount of metal adsorbed at time  $t$  (min);  $c_0$  (mg g<sup>-1</sup> min<sup>-1</sup>) is the zero-order rate constant;  $c_1$  (mg g<sup>-1</sup> min<sup>-1</sup>) is the first-order rate constant;  $c_2$  (g mg<sup>-1</sup> min<sup>-1</sup>) is the second-order rate constant;  $c_3$  (mg g<sup>-1</sup> min<sup>-1</sup>) is the pseudo first-order rate constant;  $c_4$  (g mg<sup>-1</sup> min<sup>-1</sup>) is the pseudo second-order rate constant;  $\alpha$  (mg g<sup>-1</sup> min<sup>-1</sup>) is the initial adsorption rate;  $\beta$  (g mg<sup>-1</sup>) is the extent of surface coverage and activation energy for chemisorption;  $k_{id}$  (mg g<sup>-1</sup> min<sup>-0.5</sup>) is the intraparticle diffusion rate constant;  $k_0$  (mg g<sup>-1</sup>) is the boundary layer thickness.

doses (1-7 g/L) were amended with 50 ppm of Cr (VI) in aqueous solutions. The rate of adsorption was monitored at the following optimum conditions: pH 3, 30 °C, and contact time of 75 min.

### Kinetic Profile

Rate and controlling steps are important in defining and identifying the adsorption mechanism in the system. Several kinetic models were used to capture these factors affecting adsorption using the obtained experimental data. The rate and mechanism of adsorption in this study were investigated using the zero-order, first-order, second-order, pseudo first-order, pseudo second-order, Elovich, and intra particle diffusion kinetic models.

### Statistical and Numerical Analyses

Parameters of the nonlinear models were obtained using the respective corresponding linearized forms (Table 1). Due to the linearization employed, assessment on the adequacy of the model to offer the best fit, criteria such as coefficient of determination ( $R^2$ ) and sum of squares of the error (SSE) values were employed in the selection of the best model. All statistical and numerical analyses

were performed at 5% level of significance using Microsoft Excel® and Statistical Analysis System® (SAS).

## RESULTS AND DISCUSSION

### Batch Adsorption Studies

#### Effect of pH

The optimum pH for the Cr(VI) adsorption is at pH 3 (Figure 1a). The pH is a very important parameter because it determines the speciation of the Cr(VI) ions and the surface charge of the adsorbent. The rapid decrease in adsorption at higher pH is due to the combined effect of the change in the surface charge of the adsorbent and in the shift of the Cr(VI) species in the solution<sup>19</sup>. The amine groups in the adsorbent undergo protonation and deprotonation which results in positive or negative charged surface<sup>20</sup>. The equilibrium constant for the protonation of amine groups is 6.3-7.2<sup>21</sup> with 90% of the amine groups are protonated at pH 5 and around 20% are protonated at pH 6.9. The point of zero net charge (PZNC) of the chitosan determines the exchange properties of the adsorbent. The PZNC of chitosan crosslinked with epichlorohydrin was

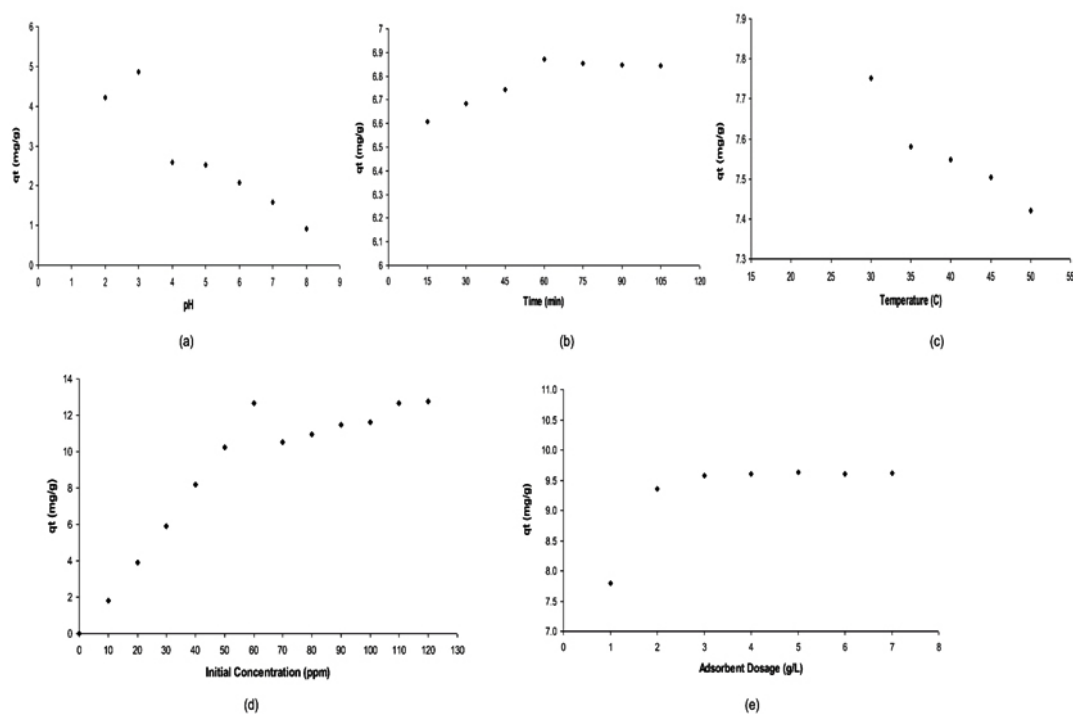


**Fig. 1: Adsorption capacity at varying (a) pH, (b) contact time, (c) temperature, (d) initial metal concentration, and (e) adsorbent dosage.**

determined to be at pH 6.75<sup>22</sup>. This study determined the PZNC of the adsorbent at pH 6.69. The charge of the adsorbent is positive when the pH is below the PZNC and conversely, negative when the pH is above the PZNC. Cr(VI) is favorably adsorbed at low pH because of its anionic property. At equilibrium,  $K_2Cr_2O_7$  dissociates into  $H_2CrO_4$ ,  $HCrO_4^{1-}$ ,  $Cr_2O_7^{2-}$ , and  $CrO_4^{2-}$  in water. The bivalent  $CrO_4^{2-}$  neutralizes twice the number of sites in the adsorbent resulting in decreased adsorption<sup>23</sup>.

**Table 2. Parameter estimates and error analysis of the different kinetic models**

Kinetic Model	Parameter	Estimates
Zero-order	$c_o$	0.0395
	$q_o$	3.8581
	$R^2$	0.3659
	SSE	25.5333
First-order	$c_1$	0.0005
	$q_o$	6.6145
	$R^2$	0.7491
	SSE	8.32e-5
Second-order	$c_2$	6.03e-5
	$q_o$	6.6138
	$R^2$	0.7494
	SSE	7.67e-6
Pseudo first-order	$q_e$ (observed)	6.8710
	$q_e$ (predicted)	0.2030
	$c_3$	0.0309
	$R^2$	0.2174
	SSE	4.0952
Pseudo second-order	$q_e$ (observed)	6.8710
	$q_e$ (predicted)	6.9061
	$c_4$	0.1839
	$R^2$	0.9999
	SSE	0.0095
Elovich	$\alpha$	2.24e18
	$\beta$	7.1023
	$R^2$	0.8826
	SSE	0.0074
Intraparticle diffusion	$k_{id}$	0.0414
	$k_o$	6.4701
	$R^2$	0.8318
	SSE	0.0106

$R^2$ : coefficient of determination; SSE: sum of squares of the error

### Effect of Contact Time

The optimum contact time was identified at 75 min (Figure 1b). Cr(VI) uptake was rapid for the first 15 min, and then proceeded at a slower rate and finally attained equilibrium after 75 min. The initial rapid rate of adsorption can be explained by the availability of free adsorption sites in the adsorbent. Initially, the surface of the adsorbent readily adsorbs the ions in the solution and over time, more of the free metal ions are adsorbed until it reaches saturation. Decrease in the rate and eventually reaching equilibrium adsorption suggests possible saturation of adsorbent or due to the electrostatic hindrance caused by the adsorbed ions<sup>24</sup>.

### Effect of Temperature

The optimum temperature for the adsorbent is 30 °C (Figure 1c). The decrease in adsorption with increasing temperature is due to the exothermic nature of the adsorption process. Heat also increases the kinetic energy of the system that leads to desorption.

### Effect of Initial Metal Concentration

The optimum metal concentration is 60 ppm (Figure 1d). At equilibrium, the surface of the adsorbent is saturated with the adsorbed Cr(VI) ions limiting further transfer of Cr(VI) ions to the surface of the adsorbent. Excess metal ion concentration in the solution at higher concentration than the optimum was not adsorbed due to the limited number of adsorption sites.

### Effect of Adsorbent Dosage

Results showed that the optimum adsorbent dosage is 3 g/L (Figure 1e). Increasing the amount of adsorbent resulted in increase of adsorption sites thus allowing more metal ions to be adsorbed. However, once equilibrium is reached, all of the metal ions were already bound to the adsorbent. There are no excess Cr(VI) in the solution, thus no further adsorption of the Cr(VI) will occur.

### Kinetic Profile

The removal of Cr(VI) continues to increase which is a typical phenomenon in any adsorption study due to the presence of several surface sorption sites as contact time increases (Figure 2a). The mean uptake of Cr(VI) showed a relatively fast initial rate on the first 20 min. which is similar to the rapid

initial adsorption of congo red taking place within the first 20-min. interval using chitosan<sup>25</sup>. Moreover, the uptake of Cr(VI) increases up to a certain threshold and then remains almost unchanged possibly due to the presence of repulsive forces between adsorbate molecules on the solid and bulk phases contributing to the observed moderate rates of adsorption as it approaches the equilibrium<sup>26</sup>. Adsorption curves are single, smooth, and continuous leading to saturation and indicate the possible monolayer coverage<sup>26, 27</sup> on the surface of adsorbents by Cr(VI). Due to the rapid adsorption of all available sites and a relatively small amount of adsorbent used, removal efficiency of Cr(VI) decreased, an increase in the amount of adsorbent may therefore reverse adsorption trend<sup>28</sup>. The percentage removal of Cr(VI) remarkably increases at an increasing dose until 3 g possibly explained by the increase in the surface area for the metal to bind with the available additional sorption sites<sup>26, 28, 29</sup>.

Parameter estimates of the different nonlinear kinetic models employed in this study were obtained using the respective linearized form of the equations (Table 1). In the zero-order kinetic model, linear plot of  $q_t$  against  $t$  was examined (Figure 2a).

With the inherent nonlinear nature of the adsorption process, parameters of this linear relationship are inadequate to capture the kinetic process as justified by the coefficient of determination significantly deviating from unity and relatively large residual error in the fit of the model (Table 2). Parameters of the first-order and second-order kinetic models were obtained by examining the linear plots of  $\log q_t$  against  $t$  (Figure 2b) and  $-1/q_t$  against  $t$  (Figure 2c), respectively. These parameters resulted to relatively small residual error values when fitted using the observed experimental data. However, the adequacy of the fit of the models is insufficient due to almost 75% coefficient of determination (Table 2).

The linear plot of  $\log(q_e - q_t)$  against  $t$  was examined in the pseudo first-order kinetic model (Figure 2d). Apparently, the relationship is not captured by the pseudo first-order mechanism as reflected by a very low coefficient of determination and significant deviation between the experimental and predicted equilibrium values ( $q_e$ ) (Table 2). Parameter estimates of the pseudo second-order kinetic model were obtained from the linear plots of  $t/q_t$  against  $t$  (Figure 2e). The obtained predicted equilibrium estimate,  $q_e$ , and the observed value

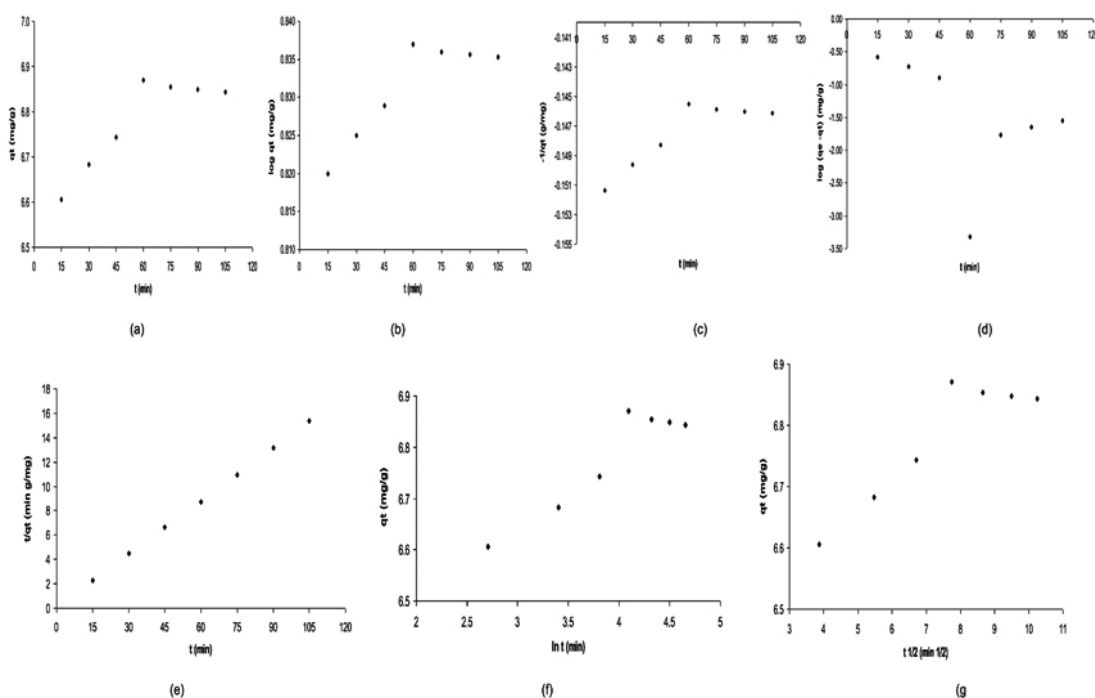


**Fig. 2:** Scatter plot of (a)zero-order, (b)first-order, (c)second-order, (d)pseudo first-order, (e) pseudo second-order, (f)Elovich, and (g)intraparticle diffusion kinetic model.

in the pseudo second-order biosorption kinetic model are almost the same, with coefficient of determination close to unity ( $R^2=0.9999$ ) which strongly suggests that the adsorption phenomenon can be modelled approximately using the pseudo second-order kinetic equation. The equilibrium system capacity obtained in the pseudo second-order is relatively more reasonable compared to the pseudo first-order when predicted results were compared with experimental measurements. The pseudo second-order model provides the best correlation in the system processes indicating that the overall rate of Cr(VI) adsorption is governed by the chemical process in accordance with the pseudo second-order reaction mechanism.

The parameter estimates of the Elovich and intraparticle diffusion models were obtained from the linear plots of  $q_t$  against  $t$  (Figure 2f) and  $q_t$  against  $t^{1/2}$  (Figure 2g), respectively. Parameter estimates of the Elovich model suggest high initial adsorption rate, extent of surface coverage, and activation energy (Table 2). The adequacy of Elovich model to fit experimental data ( $R^2=0.8826$ ) to heterogeneous catalyst surfaces helps to explain the fit in predicting the adsorption of Cr(VI) resulting to different activation energies for chemisorption. Moreover, intraparticle diffusion model offers a relatively adequate fit for the experimental data ( $R^2=0.8318$ ) as reflected by the estimates for the diffusion rate constant,  $k_{tp}$  and the thickness of boundary layer,  $k_o$  (Table 2).

Identifying the best-fit kinetic model is important in predicting the mechanisms involving

chemical reaction or mass transport process that control the rate of the pollutant removal since this information is important in the design of appropriate sorption treatment plants<sup>26</sup>. In this study, the best-fit kinetic model is the pseudo second-order equation. Although, the adsorption process is influenced by intraparticle diffusion, it is a combination of physisorption and chemisorption processes.

## CONCLUSION

Preparation of a low-cost method of activated biocharcoal-chitosan composite crosslinked with epichlorohydrin from lumbang (*Aleurites moluccana*) is successful. The optimization of the adsorption of Cr(VI) ions by the adsorbent was done by assessing the effects of pH, contact time, metal concentration, adsorbent dosage, and temperature. The synthesized composite adsorbed Cr(VI) at the optimized condition of pH 3, contact time of 75 min, metal concentration of 50 ppm, adsorbent dosage of 3 g/L, temperature of 30 °C, and agitation speed of 160 rpm. The experimental data were fitted into different adsorption kinetic models and the biosorption phenomenon behaved under a pseudo second-order rate kinetics.

## ACKNOWLEDGMENT

This work was funded by the UP System Enhanced Creative Work and Research Grant (ECWRG-2015-2-021).

## REFERENCES

1. Nriagu, J.O. Mercury pollution from the past mining of gold and silver in the Americas. *The Science of the Total Environment*. **1994**, *149*, 167-181.
2. Chung, J.Y.; Yu, S.D.; Hong, Y.S. Environmental source of arsenic exposure. *J Prev Med Public Health*. **2014**, *47*(5), 253–257.
3. Kovarik, W. Leaded gasoline: how a classic occupational disease became an international public health disaster. *Int J Occup Environ Health*. **2005**, *11*, 384–397.
4. Jarup, L. Hazards of heavy metal contamination. *British Medical Bulletin*. **2003**, *68*(1), 167-182.
5. Babel, S.; Kurniawan, T.A. Cr(VI) removal from synthetic wastewater using coconut shell charcoal and commercial activated carbon modified with oxidizing agents and/or chitosan. *Chemosphere*. **2004**, *54*, 951–967.
6. Vignati, D.A.; Dominik, J.; Beye, M.L.; Pettine, M.; Ferrari, B.J. Chromium(VI) is more toxic than chromium(III) to freshwater algae: a paradigm to revise? *Ecotoxicol Environ Saf.*

- 2010**, *73*(5), 743-749.
7. Lalvani, S.; Wiltowski, T.; Hübner, A.; Weston, A.; Mandich, N. Removal of hexavalent chromium and metal cations by a selective and novel carbon adsorbent. *Carbon*. **1998**, *36*(7-8), 1219-1226.
  8. De Mattia, G.; Bravi, M.C.; Laurenti, O.; De Luca, O.; Palmeri, A.; Sabatucci, A.; Mendico, G.; Ghiselli, A. Impairment of cell and plasma redox state in subjects professionally exposed to chromium. *Am. J. Ind. Med.* **2004**, *46*(2), 120-125.
  9. Wuana, R.A.; Okieimen, F.E. Heavy metals in contaminated soils: a review of sources, chemistry, risks and best available strategies for remediation. *ISRN Ecology*. **2011**.
  10. Barakat, M.A. New trends in removing heavy metals from industrial wastewater. *Arabian Journal of Chemistry*. **2011**, *4*(4), 361-377.
  11. Kulkarni, S.; Kaware, J. Regeneration and recovery in adsorption: A review. *International Journal of Innovative Science, Engineering & Technology*. **2014**, *1*(8), 61-64.
  12. Chen, A.; Liu, S.; Chen, C.; Chen, C. Comparative adsorption of Cu(II), Zn(II), and Pb(II) ions in aqueous solution on the crosslinked chitosan with epichlorohydrin. *Journal of Hazardous Materials*. **2008**, *154*(1-3), 184-191.
  13. Cheung, R.C.F.; Ng, T.B.; Wong, J.H.; Chan, W.Y. Chitosan: an update on potential biomedical and pharmaceutical applications. *Mar Drugs*. **2015**, *13*(8), 5156-5186.
  14. Laus, R.; Costa, T.; Szpoganicz, B.; Fávère, V. Adsorption and desorption of Cu(II), Cd(II) and Pb(II) ions using chitosan crosslinked with epichlorohydrin-triphosphate as the adsorbent. *Journal of Hazardous Materials*. **2010**, *183*(1-3), 233-241.
  15. Hydari, S.; Sharififard, H.; Nabavinia, M.; Parvizi, M. A comparative investigation on removal performances of commercial activated carbon, chitosan biosorbent and chitosan/activated carbon composite for cadmium. *Chemical Engineering Journal*. **2012**, *193-194*, 276-282.
  16. Sharififard, H.; Ashtiani F.Z.; Soleimani M. Adsorption of palladium and platinum from aqueous solutions by chitosan and activated carbon coated with chitosan. *Asia-Pac. J. Chem. Eng.* **2012**.
  17. Clesceri, L.S.; Greenberg, A.E.; Eaton, A.D. Standard methods for the examination of water and waste water. American Public Health Association, Washington. **1998**, *20<sup>th</sup> Ed.*
  18. Chakravarty, S.; Dureja, V.; Bhattacharyya, G.; Maity, S.; Bhattacharjee, S. Removal of arsenic from groundwater using low cost ferruginous manganese ore. *Water Research*. **2002**, *36*(3), 625-632.
  19. Harter, R.; Naidu, R. An assessment of environmental and solution parameter impact on trace-metal sorption by soils. *Soil Sci. Soc. Am. J.* **2001**, *65*, 597-612.
  20. Gerente, C.; Lee, V. K. C.; Cloirec, P.; McKay, G. Application of chitosan for the removal of metals from wastewaters by adsorption—mechanisms and models review. *Critical Reviews in Environmental Science and Technology*, **2007**, *37*(1), 41-127.
  21. Kakavandi, B.; Kalantary, R. R.; Jafari, A. J.; Nasser, S.; Ameri, A.; Esrafil, A.; Azari, A. Pb(II) adsorption onto a magnetic composite of activated carbon and superparamagnetic Fe<sub>3</sub>O<sub>4</sub> nanoparticles: Experimental and modeling study. *CLEAN - Soil, Air, Water*, **2015**, *43*(8), 1157-1166.
  22. Copello, G. J.; Villanueva, M. E.; Gonzalez J. A.; Egues, S.; Diaz, L.E. TEOS as an improved alternative for chitosan beads cross-linking: a comparative adsorption study. *Journal of Applied Polymer Science*. **2014**, *131*(21), 1-8.
  23. Pandey, P.K.; Sharma, S.K.; Sambhi, S.S. Kinetics and equilibrium study of chromium adsorption on zeolite NaX. *International Journal of Environmental Science & Technology*. **2010**, *7*(2), 395-404.
  24. Goswami, A.; Raul, P.K.; Purkait, M.K. Arsenic adsorption using copper (II) oxide nanoparticles. *Chem. Eng. Res. Des.* **2012**.
  25. Jabbar, A. Z.; Hadi, A.G.; Sami, F. Removal of azo dye from aqueous solution using chitosan. *Orient. J. Chem.* **2014**, *30*(2), 571-575.
  26. Sumalapao, D.E.P.; Distor, J.R.; Domingo, N.T.S.; Dy, L.F.; Villarante, N.R. Biosorption kinetic models on the removal of congo red onto unripe calamansi (*Citrus microcarpa*) peels. *Orient. J. Chem.* **2016**, *32*(6), 2889-

- 2900.
27. Mane, V.S.; Mall, I.D.; Srivastava, V.C. Use of bagasse fly ash as an adsorbent for the removal of brilliant green dye from aqueous solution. *Dyes and Pigments*. **2007**, *73*(3), 269-278.
28. Ayawei, N.; Ekubo, A.T.; Wankasi, D.; Dikio, E.D. Adsorption of congo red by Ni/Al-CO<sub>3</sub>: Equilibrium, Thermodynamic, and Kinetic Studies. *Orient .J.Chem.* **2015**, *31*(3), 1307-1308.
29. Wong, Y.C.; Ranjini, K.N.; Wan-Nurdiyana, W.A. Removal of congo red and acid yellow 36 dye using orange peel and rice husk as absorbents. *Orient .J.Chem.* **2014**, *30*(2), 529-539.